

# The Method of Fundamental Solutions for General Orthotropic Elastic Problems

Zhaoyang Wang and Yan Gu\*

College of Mathematics, Qingdao University, Qingdao 266071, PR China

## Abstract

In this communication we investigate the application of the method of fundamental solutions (MFS) for the solution of plane orthotropic elastic problems. The displacements and stresses are approximated by linear combinations of the fundamental solutions of the Navier-Cauchy equations for orthotropic materials. The numerical results obtained illustrate that the MFS is accurate, convergent, and computational efficient, and thence it could be considered as a competitive alternative to existing methods for solving orthotropic elastic problems.

## Publication History:

Received: January 28, 2016

Accepted: September 19, 2016

Published: September 21, 2016

## Keywords:

Method of fundamental solutions, Meshless boundary collocation method, Elasticity, Orthotropic materials

## Introduction

The method of fundamental solutions (MFS) may be seen as one of the simplest methods for the numerical solution of certain boundary value problems [1-5]. It belongs to the family of meshless boundary collocation methods that may present remarkable results with a small computational effort. In the MFS, the solution of a given problem is approximated by a linear combination of the fundamental solutions with the sources located outside the solution domain. The advantages that the MFS has over the more classical domain or boundary discretization methods can be summarized as follows. First of all, it is a boundary-type method which means that it shares the same advantages of the boundary element method (BEM) has over domain discretization methods. Secondly, it is meshless and does not require the task of domain and/or boundary meshing which can be arduous, time-consuming and computationally expensive for methods needing for meshing. Thirdly, it does not involve costly integrations which could be otherwise troublesome as in the case, for example, the BEM-based methods. These features make the method very easy to implement, in particular for problems in complex geometries and high dimensions. Some surveys of the MFS and its application for the numerical solutions of elliptic boundary value problems are available in Refs. [6-9]. In recent years a few different meshless boundary discretization techniques which are different but also high related to the MFS have been proposed and used successfully, see for example the singular boundary method (SBM) [10-13].

The objective of this communication is to make the first attempt to extend the MFS for the solution of general orthotropic elastic problems. The displacements and stresses are approximated by using linear combinations of the fundamental solutions of the Navier-Cauchy equations for orthotropic materials. The paper is organized as follows: the governing equations and the MFS formulation for orthotropic elastic problems are presented in Section 2, followed in Section 3 three benchmark numerical examples are well studied to illustrate the accuracy and efficiency of the method. Finally, the conclusions and remarks are provided in Section 4.

## Governing Equations and The MFS Formulation for Orthotropic Elastic Problems

For the assumption of plane stress distribution in an orthotropic material, Hooke's law takes the form (matrix representation)

$$\begin{bmatrix} \varepsilon_x \\ \varepsilon_y \\ \gamma_{xy} \end{bmatrix} = \begin{bmatrix} S_{11} & S_{12} & 0 \\ S_{21} & S_{22} & 0 \\ 0 & 0 & S_{66} \end{bmatrix} \begin{bmatrix} \sigma_x \\ \sigma_y \\ \tau_{xy} \end{bmatrix} = \begin{bmatrix} 1/E_1 & -\nu_{12}/E_1 & 0 \\ -\nu_{12}/E_1 & 1/E_2 & 0 \\ 0 & 0 & 1/G_{12} \end{bmatrix} \begin{bmatrix} \sigma_x \\ \sigma_y \\ \tau_{xy} \end{bmatrix} \quad (1)$$

where the stress  $\sigma_{ij}$  and strain  $\varepsilon_{ij}$  are mean values taken through the thickness of the material;  $S_{ij}$  ( $i, j=1, 2$ ) and  $S_{66}$  are flexibility coefficients;  $E_1$  and  $E_2$  are Young's moduli in the directions of  $x_1$  and  $x_2$  axes;  $G_{12}$  denotes the shear modulus for planes parallel to the  $x_1 - x_2$  plane;  $\nu_{12}$  is Poisson's ratio characterizing the contraction in the direction of the axis when tension is applied in the direction of the axis. The Navier-Cauchy equations for plane orthotropic materials [14], in the absence of body forces, referring to displacements  $u_i$  and  $u_i$  are

$$C_{11} \frac{\partial^2 u_1(\mathbf{x})}{\partial x_1^2} + (C_{12} + C_{66}) \frac{\partial^2 u_2(\mathbf{x})}{\partial x_1 \partial x_2} + C_{66} \frac{\partial^2 u_1(\mathbf{x})}{\partial x_2^2} = 0 \quad (2)$$

$$C_{22} \frac{\partial^2 u_2(\mathbf{x})}{\partial x_2^2} + (C_{12} + C_{66}) \frac{\partial^2 u_1(\mathbf{x})}{\partial x_1 \partial x_2} + C_{66} \frac{\partial^2 u_2(\mathbf{x})}{\partial x_1^2} = 0 \quad (3)$$

in which  $C_{11}=S_{12}/D$ ,  $C_{12}=-S_{12}/D$ ,  $C_{22}=-S_{11}/D$ ,  $C_{66}=1/S_{66}$ ,  $D=S_{11}S_{22}-S_{12}^2$

These are subject to the boundary conditions

$$u_i(\mathbf{x}) = \bar{u}_i \quad \mathbf{x} \in \Gamma_u \text{ (Dirichlet boundary conditions)} \quad (4)$$

$$t_i(\mathbf{x}) = \bar{t}_i \quad \mathbf{x} \in \Gamma_t \text{ (Neumann boundary conditions)} \quad (5)$$

where  $t_i(x)$  denotes the component of boundary traction in the  $i^{\text{th}}$  coordinate direction,  $\Gamma_u$  and  $\Gamma_t$  construct the whole boundary of the domain  $\Omega$  which we shall assume to be piecewise smooth,  $u_i$  and  $t_i$  represent the prescribed displacements and tractions, respectively.

Employing indicial notation for the coordinates of points  $\mathbf{x}$  and  $\mathbf{y}$ , i.e.  $x_1, x_2$  and  $y_1, y_2$ , respectively, the Kelvin fundamental solutions of the systems (2) and (3) can be expressed as [14]

**Corresponding Author:** Prof. Yan Gu, College of Mathematics, Qingdao University, Qingdao 266071, PR China, E-mail: [guyan1913@163.com](mailto:guyan1913@163.com)

**Citation:** Wang Z, Gu Y (2016) The Method of Fundamental Solutions for General Orthotropic Elastic Problems. Int J Appl Exp Math 1: 109. doi: <http://dx.doi.org/10.15344/ijaem/2016/109>

**Copyright:** © 2016 Wang et al. This is an open-access article distributed under the terms of the Creative Commons Attribution License, which permits unrestricted use, distribution, and reproduction in any medium, provided the original author and source are credited.

$$U_{11}(\mathbf{y}, \mathbf{x}) = K \left[ \sqrt{\alpha_1} A_2 \ln r_1 - \sqrt{\alpha_2} A_1 \ln r_2 \right] \quad (6a)$$

$$U_{12}(\mathbf{y}, \mathbf{x}) = -K A_1 A_2 \left[ \arctan \frac{x_2 - y_2}{\sqrt{\alpha_1} (x_1 - y_1)} - \arctan \frac{x_2 - y_2}{\sqrt{\alpha_2} (x_1 - y_1)} \right] \quad (6b)$$

$$U_{21}(\mathbf{y}, \mathbf{x}) = U_{12}(\mathbf{y}, \mathbf{x}) \quad (6c)$$

$$U_{22}(\mathbf{y}, \mathbf{x}) = K \left[ A_2^2 \ln r_2 / \sqrt{\alpha_2} - A_1^2 \ln r_1 / \sqrt{\alpha_1} \right] \quad (6d)$$

where  $\alpha_1$  and  $\alpha_2$  satisfy

$$\alpha_1 + \alpha_2 = (2S_{12} + S_{66}) / S_{22}, \quad \alpha_1 \alpha_2 = S_{11} / S_{22}$$

and

$$K = 1 / [2\pi(\alpha_1 - \alpha_2)S_{22}]$$

$$A_i = S_{12} - \alpha_i S_{22}$$

$$r_i = \sqrt{\alpha_i (x_1 - y_1)^2 + (x_2 - y_2)^2}$$

The fundamental solution  $U_{ij}(\mathbf{y}, \mathbf{x})$  described above indicates the displacement produced at the point  $\mathbf{y}$  by a concentrated unit body force applied at the point  $\mathbf{x}$ , in which the first subscript ( $i$ ) denotes the direction of the displacement whereas the second one ( $j$ ) the direction of the unit force. The fundamental solution of the tractions can be obtained by first calculating the fundamental solutions of strains and then applying Hooke's law

$$T_{11}(\mathbf{y}, \mathbf{x}) = K [(x_1 - y_1)n_1(\mathbf{y}) + (x_2 - y_2)n_2(\mathbf{y})] \left[ \frac{A_2 \sqrt{\alpha_1}}{r_1^2} - \frac{A_1 \sqrt{\alpha_2}}{r_2^2} \right] \quad (7d)$$

$$T_{12}(\mathbf{y}, \mathbf{x}) = K \frac{A_2}{r_2^2} \left[ \sqrt{\alpha_2} (x_1 - y_1)n_2(\mathbf{y}) - (x_2 - y_2)n_1(\mathbf{y}) / \sqrt{\alpha_2} \right] - K \frac{A_1}{r_1^2} \left[ \sqrt{\alpha_1} (x_1 - y_1)n_2(\mathbf{y}) - (x_2 - y_2)n_1(\mathbf{y}) / \sqrt{\alpha_1} \right] \quad (7b)$$

$$T_{21}(\mathbf{y}, \mathbf{x}) = K \frac{\alpha_2 A_1}{r_2^2} \left[ \sqrt{\alpha_2} (x_1 - y_1)n_2(\mathbf{y}) - (x_2 - y_2)n_1(\mathbf{y}) / \sqrt{\alpha_2} \right] - K \frac{\alpha_1 A_2}{r_1^2} \left[ \sqrt{\alpha_1} (x_1 - y_1)n_2(\mathbf{y}) - (x_2 - y_2)n_1(\mathbf{y}) / \sqrt{\alpha_1} \right] \quad (7c)$$

$$T_{22}(\mathbf{y}, \mathbf{x}) = K [(x_1 - y_1)n_1(\mathbf{y}) + (x_2 - y_2)n_2(\mathbf{y})] \left[ \frac{A_2 \sqrt{\alpha_2}}{r_2^2} - \frac{A_1 \sqrt{\alpha_1}}{r_1^2} \right] \quad (7d)$$

The displacements can be approximated by linear combinations of fundamental solutions with respect to different source points  $\mathbf{x}$  as follows:

$$u_1(\mathbf{y}) = \sum_{j=1}^N [a_j U_{11}(\mathbf{y}, \mathbf{x}^j) + b_j U_{12}(\mathbf{y}, \mathbf{x}^j)] \quad (8a)$$

$$u_2(\mathbf{y}) = \sum_{j=1}^N [a_j U_{21}(\mathbf{y}, \mathbf{x}^j) + b_j U_{22}(\mathbf{y}, \mathbf{x}^j)] \quad (8b)$$

and the tractions are approximated accordingly. In the above equations,  $N$  is the specified number of sources,  $\mathbf{y} \in \bar{\Omega} = \Omega \cup \partial\Omega$  is collocation points,  $\{a_j\}_{j=1}^N$  and  $\{b_j\}_{j=1}^N$  denote the unknown coefficients, and  $\mathbf{x}^j$  stands for the  $j^{\text{th}}$  source point, which lies outside  $\bar{\Omega}$ . In the MFS, the source points  $\mathbf{x}$  are either pre-assigned or taken to be part of the unknowns of the problem along with the coefficients  $\{a_j\}_{j=1}^N$  and  $\{b_j\}_{j=1}^N$ . In either case, the unknowns are determined so that the approximations (8) satisfy, in some sense, the boundary conditions (4) and (5) as well as possible [15, 16]. Usually, this is done by collocating the boundary conditions at a chosen set of boundary points  $\{\mathbf{y}^i\}_{i=1}^M$ . In this work, for simplicity the locations of the source points are pre-assigned, taken to be a curve similar to the real boundary, and assume that the number

of source points is equal to that of collocation points. Once all coefficients are computed, the displacements and stresses at any point inside the domain can be obtained directly from Eqs. (8) and (9):

$$\sigma_{11}(\mathbf{y}) = \sum_{j=1}^N [a_j D_{111}(\mathbf{y}, \mathbf{x}^j) + b_j D_{112}(\mathbf{y}, \mathbf{x}^j)] \quad (9a)$$

$$\sigma_{12}(\mathbf{y}) = \sum_{j=1}^N [a_j D_{121}(\mathbf{y}, \mathbf{x}^j) + b_j D_{122}(\mathbf{y}, \mathbf{x}^j)] \quad (9b)$$

$$\sigma_{22}(\mathbf{y}) = \sum_{j=1}^N [a_j D_{221}(\mathbf{y}, \mathbf{x}^j) + b_j D_{222}(\mathbf{y}, \mathbf{x}^j)] \quad (9c)$$

where

$$D_{111}(\mathbf{y}, \mathbf{x}) = K(x_1 - y_1) \left( \frac{A_2 \sqrt{\alpha_1}}{r_1^2} - \frac{A_1 \sqrt{\alpha_2}}{r_2^2} \right), \quad D_{112}(\mathbf{y}, \mathbf{x}) = K(x_2 - y_2) \left( \frac{A_1}{\sqrt{\alpha_1} r_1^2} - \frac{A_2}{\sqrt{\alpha_2} r_2^2} \right) \quad (10a)$$

$$D_{121}(\mathbf{y}, \mathbf{x}) = K(x_2 - y_2) \left( \frac{A_2 \sqrt{\alpha_1}}{r_1^2} - \frac{A_1 \sqrt{\alpha_2}}{r_2^2} \right), \quad D_{122}(\mathbf{y}, \mathbf{x}) = K(x_1 - y_1) \left( \frac{A_2 \sqrt{\alpha_2}}{r_2^2} - \frac{A_1 \sqrt{\alpha_1}}{r_1^2} \right) \quad (10b)$$

$$D_{221}(\mathbf{y}, \mathbf{x}) = K(x_1 - y_1) \left( \frac{A_2 \sqrt{\alpha_2}}{r_2^2} - \frac{A_1 \sqrt{\alpha_1}}{r_1^2} \right), \quad D_{222}(\mathbf{y}, \mathbf{x}) = K(x_2 - y_2) \left( \frac{A_2 \sqrt{\alpha_2}}{r_2^2} - \frac{A_1 \sqrt{\alpha_1}}{r_1^2} \right) \quad (10c)$$

are fundamental solutions of stresses. The proper location of the source points is an important issue in the MFS with respect to the accuracy of the numerical solution [17-20]. In this paper, the distance between the source points to the boundary is computed by the following equation [6]:

$$d = \lambda |\mathbf{y} - \mathbf{y}_c| \quad (11)$$

where  $\mathbf{y}_c = (y_1^c, y_2^c)$  is the coordinates of the center of the computational domain  $\lambda$  and is a pre-assigned parameter. Once the parameter  $\lambda$  is chosen, the distribution of the source points is then determined.

## Numerical Results and Discussions

### An infinite plate with a circular hole

An infinite orthotropic plate with a circular hole subjected to the uniform tensile forces at infinity is studied first, as illustrated in Figure 1. The radius of the circular hole is  $r$ . The analytical solution corresponding to this problem can be found in [21], Equation (31.11) on Page A plot of the distributed collocation and source points with the infinite plate is shown in Figure 1.

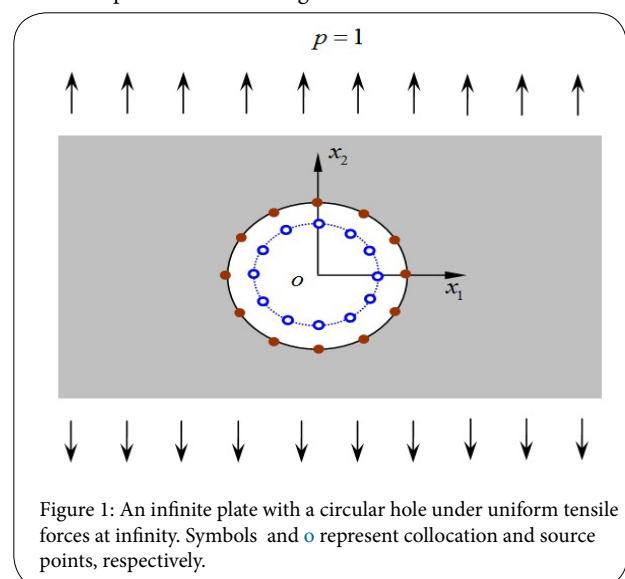


Figure 1: An infinite plate with a circular hole under uniform tensile forces at infinity. Symbols  $\bullet$  and  $\circ$  represent collocation and source points, respectively.

Here the stress of interest is that at the edge of the hole, tangential stress  $\sigma_\theta$ , where, as a number of solved problems show, it is the greatest. Figure 2 illustrates the variation of the stress  $\sigma_\theta$  along the edge of the hole for two different orthotropic materials. For the numerical implementation,  $N=200$  evenly distributed source points are chosen along the boundary and the distance between the fictitious boundary and the real boundary is taken to be  $\lambda=0.2$ , i.e., As shown in Figure 2, the results predicted by the MFS are in quite good agreement with the analytical solutions. This figure also illustrates that, for orthotropic materials, of all possible tangential stresses the greatest one occurs in the case that the tension is applied in a direction for which Young's modulus is maximum, which is quite different from the isotropic material. In such case the maximum stress in an orthotropic plate ( $\sigma_{max}=3.067$ ) is greater than that in a similar isotropic plate ( $\sigma_{max}=3$ ). Furthermore, for all cases discussed here the most severely stressed regions, as would be expected, are near the point (1,0) (the angular distance from this point does not exceed  $10^\circ$ ).

where  $I_{numerical}^k$  and  $I_{exact}^k$  denote the numerical and analytical solutions at the  $k$ th calculated point, respectively. As Table 1 shows, the MFS results agree pretty well with the analytical solution when the value of the ratio changes from 0.1 to 0.9. Beyond this range the numerical accuracy is found to be less satisfactory.

**Normal pressure distributed uniformly along the edge of a hole**

As a further illustration we consider an infinite plate with a hole subject to normal pressure distributed uniformly along the edge of the hole, as illustrated in Figure 3(a). The radius of the circular hole is  $r$  and the location of the collocation and source points is the same as that distributed in preceding problem. The analytical solution corresponding to this problem can be found in [21], Equation (32.5) on Page 182.

Table 2 shows the numerical results of tangential stress  $\sigma_\theta$  distributed along the boundary, with  $S_{11}=1.61E-6$ ,  $S_{22}=1.76E-6$ ,

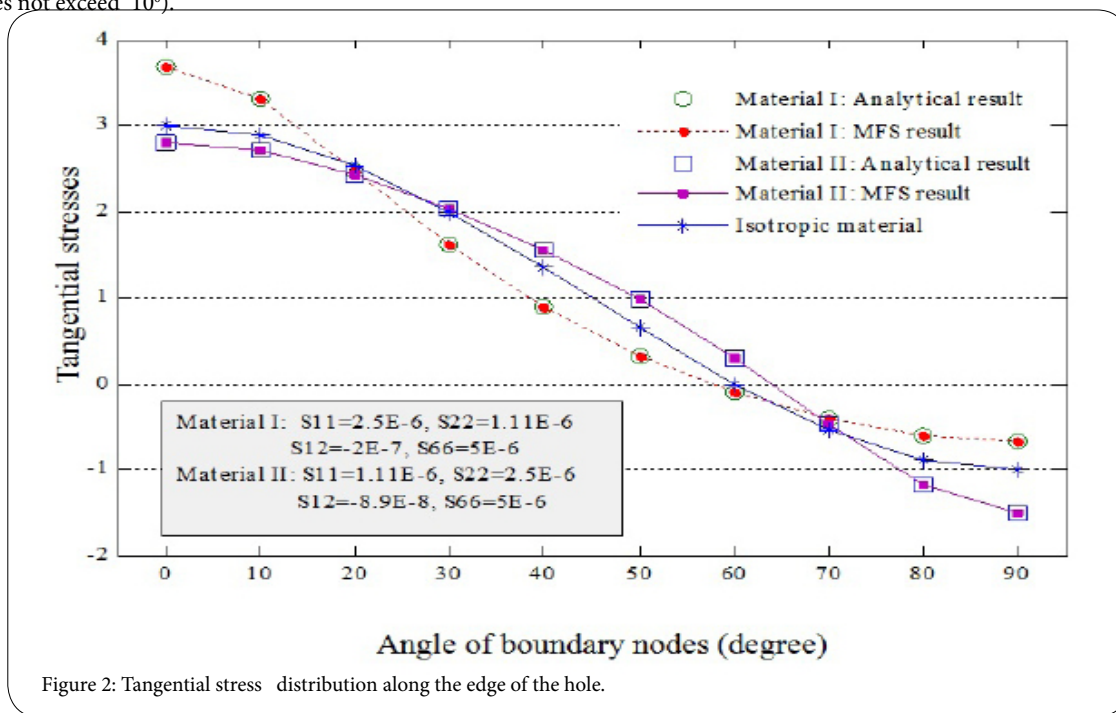


Figure 2: Tangential stress distribution along the edge of the hole.

To study the sensitivity of the MFS-results with respect to the location of the fictitious boundary, Table 1 lists the relative errors of tangential stress distributed along the edge of the hole, with  $S_{11}=1.61E-6$ ,  $S_{22}=1.76E-6$ ,  $S_{66}=1.61E-7$ ,  $S_{12}=1.61E-7$ ,  $S_{66}=3.92E-6$ , and  $N=100$ . The relative error of the numerical solution is defined as

$$\text{Relative Error} = \left| \frac{I_{numerical}^k - I_{exact}^k}{I_{exact}^k} \right| \tag{12}$$

$S_{12}=-1.61E-7$ ,  $S_{66}=8.33E-6$  and  $N=300$ , and  $\lambda=2$ . We can observe that the MFS results are in consistent agreement with the analytical solution, with the largest relative error less than  $6E-6$ . Figure 3(b) plots the variation of tangential stresses around the boundary. The intensity of the stress is represented by distances outward from the circular hole along lines through the center of the hole. Note that the maximum stress occurs at regions near the direction of  $x$  and  $y$  axes, which agrees well with the distribution illustrated in [21], Figure 3.

Angle (degrees)	Location of the fictitious boundary ( $\lambda$ )								
	0.1	0.2	0.3	0.4	0.5	0.6	0.7	0.8	0.9
0	3.19E-4	9.06E-8	8.74E-10	1.55E-9	7.82E-10	2.90E-10	1.31E-7	2.57E-5	4.89E-4
30	4.23E-4	1.58E-7	9.47E-10	2.02E-9	1.06E-9	8.67E-10	2.07E-7	9.42E-5	1.82E-4
45	2.51E-3	2.56E-7	1.35E-9	1.07E-9	1.11E-9	2.16E-9	1.01E-7	5.20E-5	2.73E-3
60	8.78E-2	2.66E-5	1.05E-7	6.69E-9	4.58E-8	1.04E-7	2.54E-5	4.82E-4	6.62E-3
90	6.57E-3	2.69E-6	1.40E-9	6.97E-10	4.30E-10	1.39E-9	7.34E-7	5.19E-5	1.65E-3

Table 1: Relative errors of tangential stress along the edge of the hole as functions of various values of  $\lambda$ .

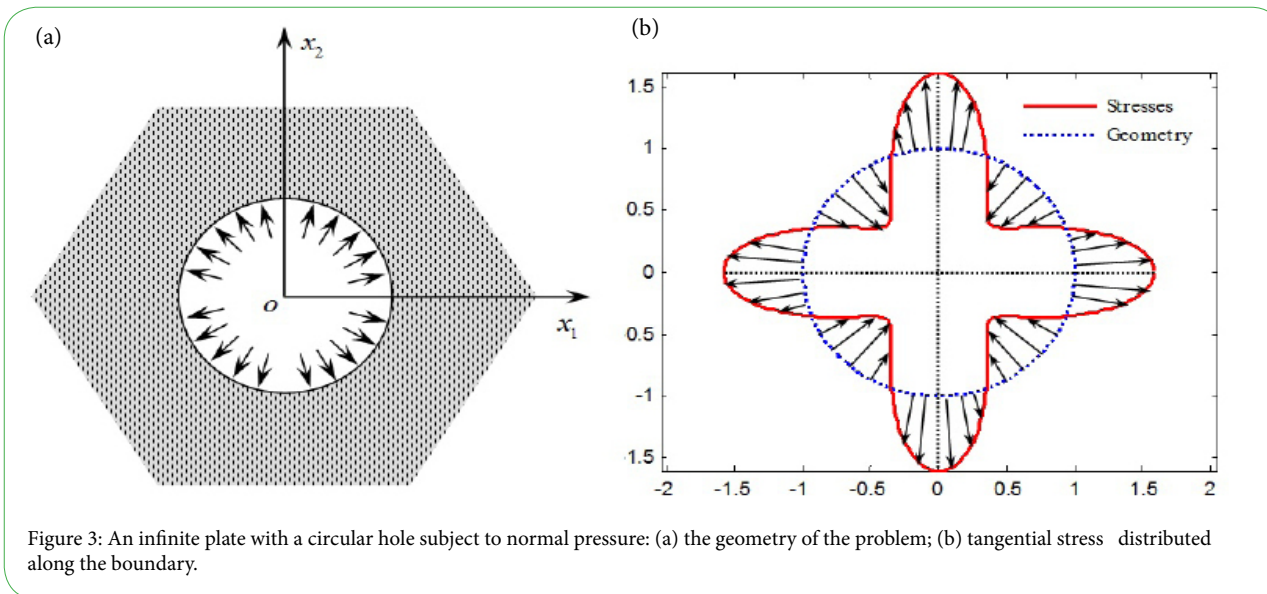


Figure 3: An infinite plate with a circular hole subject to normal pressure: (a) the geometry of the problem; (b) tangential stress distributed along the boundary.

Angle (degrees)	Exact solution	MFS results	Relative errors
0	1.585898	1.585893	2.865602E-6
30	0.722379	0.722383	5.552263E-6
45	0.539211	0.539209	3.362518E-6
60	0.705160	0.705159	1.587068E-6
90	1.612623	1.612624	3.087380E-7

Table 2: Tangential stresses along the edge of the hole.

Since analytical solutions for this problem are not available, the problem is solved for an increasing sequence of values of the outer radius with a final ratio  $r_b/r_a=2000$ . The final ratio approximates an infinite plate with a circular hole subjected to uniform normal pressure which is solved in the previous example 2. The distribution of tangential stress  $\sigma_\theta$  around the inner boundary of the cylinder is studied and three of the distributions are shown in Figure 4(b). We find that the limiting case (ratio 2000) compares well with the analytical solution.

### A thick-walled cylinder

Finally, consider the problem of a circular orthotropic ring, fixed on its outer boundary, subjected to a uniform normal pressure  $p=1$  on its inner boundary, as illustrated in Figure 4. The inner and outer radii of the cylinder are  $r_a$  and  $r_b$ , respectively. Here, each boundary is divided into 60 equal intervals, i.e.,  $N=200$ . The material constants are the same as those used in example 2.

As the number of boundary nodes increases, Figure 5 illustrates the convergence curves of the tangential stress at points along the inner boundary of the cylinder, with  $r_b/r_a=3$  and  $r_b/r_a=7$ . It can be seen that the relative errors decrease until the number of source points reaches 20, after which a further increase in the number of source points does not improve substantially the accuracy of the numerical results.

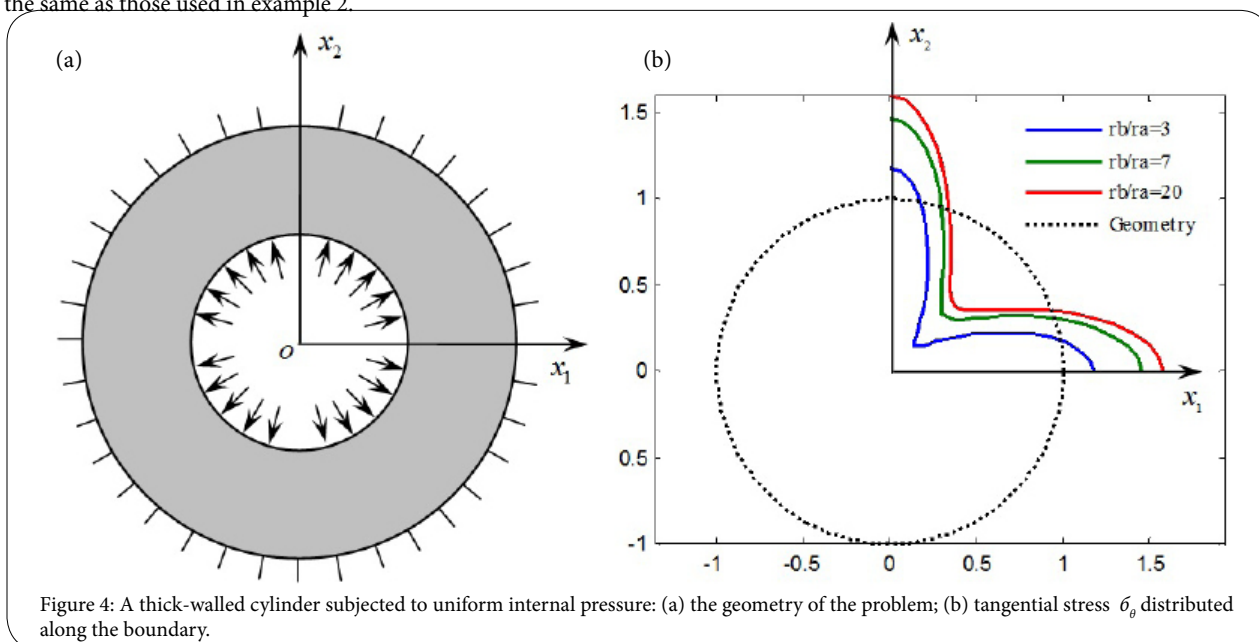


Figure 4: A thick-walled cylinder subjected to uniform internal pressure: (a) the geometry of the problem; (b) tangential stress  $\sigma_\theta$  distributed along the boundary.

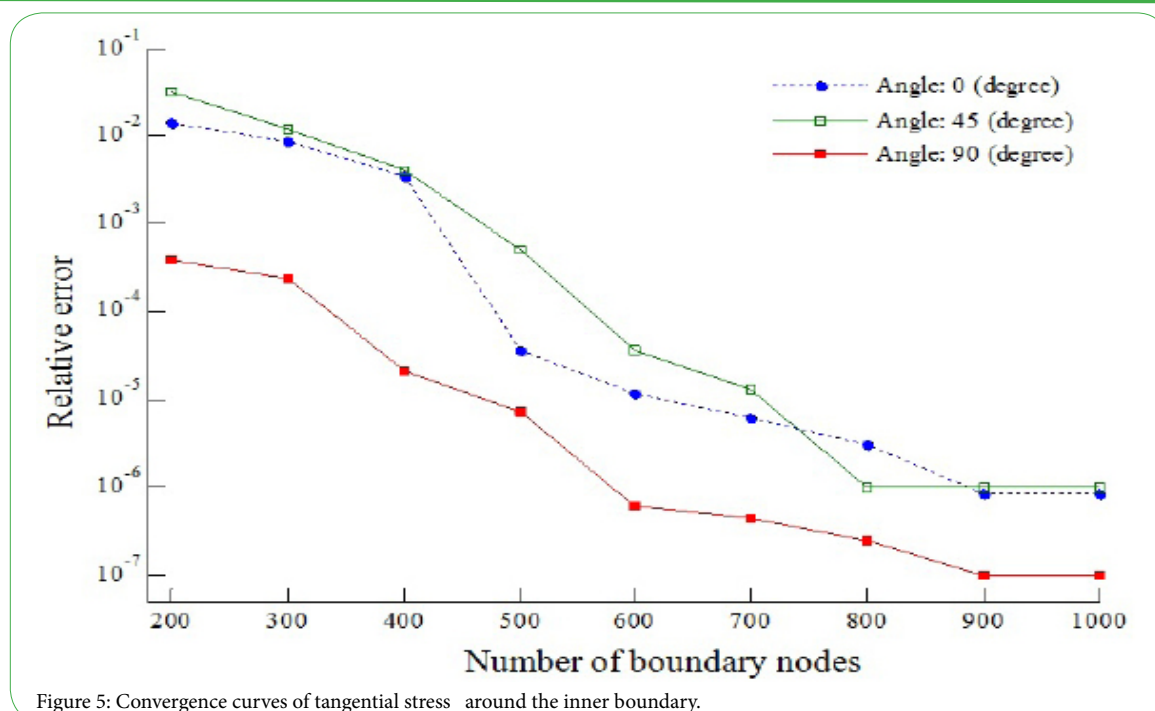


Figure 5: Convergence curves of tangential stress around the inner boundary.

## Conclusion

In this work, we describe the application of the MFS to plane orthotropic elastic problems. The method is very easy to implement, requires little data preparation, and, unlike boundary element method, it avoids potentially troublesome and costly integrations on the boundary. Numerical tests indicate that satisfactory accuracy can be obtained with relatively few degrees of freedom. In conclusion, the MFS could be considered as a competitive alternative for solving orthotropic elastic problems.

## Competing Interests

The authors declare that they have no competing interests.

## Funding

This research is supported by the National Natural Science Foundations of China (60974025, 60973048, 61272077), the Natural Science Foundation of Guangxi Autonomous Region (No. 2012GXNSFBA053003, 2013YB141).

## References

- Fairweather G, Karageorghis A (1998) The method of fundamental solutions for elliptic boundary value problems. *Adv Comput Math* 9: 69-95.
- Chen CS, Golberg MA, Hon YC (1998) The method of fundamental solutions and quasi-Monte-Carlo method for diffusion equations. *Int J Numer Methods Eng* 43: 1421-1435.
- Karageorghis A, Fairweather G (2000) The Method of Fundamental Solutions for axisymmetric elasticity problems. *Comput Mech* 25: 524-532.
- Chen CS (1995) The method of fundamental solutions for non-linear thermal explosions. *Commun Numer Methods Eng* 11: 675-681.
- Chen CS, Cho HA, Golberg MA (2006) Some comments on the ill-conditioning of the method of fundamental solutions. *Eng Anal Bound Elem* 30: 405-410.
- Young DL, Jane SJ, Fan CM, Murugesan K, Tsai CC (2006) The method of fundamental solutions for 2D and 3D Stokes problems. *J Comput Phys* 211: 1-8.
- Marin L, Lesnic D (2007) The method of fundamental solutions for nonlinear functionally graded materials. *Int J Solids Struct* 44: 6878-6890.
- Poullikkas A, Karageorghis A, Georgiou G (2002) The method of fundamental solutions for three-dimensional elastostatics problems. *Comput Struct* 80: 365-370.
- Berger JR, Karageorghis A (2001) The method of fundamental solutions for layered elastic materials. *Eng Anal Bound Elem* 25: 877-886.
- Chen W, Gu Y (2012) An improved formulation of singular boundary method. *Adv Appl Math Mech* 4: 543-558.
- Gu Y, Chen W, He XQ (2014) Improved singular boundary method for elasticity problems. *Comput Struct* 135: 73-82.
- Gu Y, Chen W, Fu ZJ, Zhang B (2014) The singular boundary method: Mathematical background and application in orthotropic elastic problems. *Eng Anal Bound Elem* 44: 152-160.
- Gu Y, Chen W, He XQ (2012) Singular boundary method for steady-state heat conduction in three dimensional general anisotropic media. *Int J Heat Mass Transf* 55: 4837-4848.
- Rizzo FJ, Shippy DJ (1970) A Method for Stress Determination in Plane Anisotropic Elastic Bodies. *J Composite Mater* 4: 36-61.
- Karageorghis A, Lesnic D (2010) The method of fundamental solutions for the inverse conductivity problem. *Inverse Probl Sci Eng* 18: 567-583.
- Johansson BT, Lesnic D, Reeve T (2012) A method of fundamental solutions for the radially symmetric inverse heat conduction problem. *Int Commun Heat Mass Transfer* 39: 887-895.
- Sarler B (2009) Solution of potential flow problems by the modified method of fundamental solutions: Formulations with the single layer and the double layer fundamental solutions. *Eng Anal Bound Elem* 33: 1374-1382.
- Alves CJS (2009) On the choice of source points in the method of fundamental solutions. *Eng Anal Bound Elem* 33: 1348-1361.
- Chen CS, Liu GR (2004) Preface to: Mesh reduction techniques--Part I. *Eng Anal Bound Elem* 28: 423-424.
- Liu YJ (2010) A new boundary mesh free method with distributed sources. *Eng Anal Bound Elem* 34: 914-919.
- Lekhnitskii SG (1963) *Theory of Elasticity of an Anisotropic Elastic Body*. Holden-Day Series in Mathematical Physics USA.